# THERMODYNAMIC SELECTION OF THE OPTIMAL WORKING FLUID

Attila R. Imre[1,2]*, Réka Kustán[1], Axel Groniewsky[1]

[1]Budapest University of Technology and Economics, Department of Energy Engineering,
Muegyetem rkp. 3, H-1111 Budapest, Hungary
imreattila@energia.bme.hu,kustan@energia.bme.hu,groniewsky@energia.bme.hu

[2]Hungarian Academy of Science, Centre for Energy Research, Department of Thermohydraulics,
POB. 49, H-1525 Budapest, Hungary

* Corresponding Author

## ABSTRACT

A novel method proposed to choose the best working fluid – from the point of view of expansion route – for a given heat source and heat sink (characterized by a maximum and minimum temperature). The method is based on the novel classification of working fluids using the sequences of their characteristic points on temperature-entropy space. The most suitable existing working fluid can be selected, where an ideal adiabatic (isentropic) expansion step between a given upper and lower temperature is possible in a way, that the initial and final states are both saturated vapour states and the ideal (isentropic) expansion line runs in the superheated (dry) vapour region all along the expansion. Problems related to the presence of droplets or superheated dry steam in the final expansion state can be avoided or minimized by using the working fluid chosen with this method. Since most of the known working fluids have optimal expansion routes at low temperatures, presently the method is most suitable to choose working fluids for cryogenic cycles, applied for example for heat recovery during LNG-regasification. Some of the materials, however, can be applied in ranges located at relatively higher temperatures, therefore the method can also be applied in some limited manner for the utilization of other low-temperature heat sources (like geothermal or waste heat) as well. Obviously, this method is limited only on one part of the multi-dimensional optimization process and therefore, in the real working fluid selection, it should be used together with other criteria.

## 1. INTRODUCTION

For conversing the heat of low-temperature heat sources to electricity, Organic Rankine Cycle (ORC) is often applied (Macchi and Astolfi, 2016, Blaise and Feidt, 2019). There are several known – and probably even more unknown – low boiling-point working fluid to be used to convert heat to work. The selection of the ideal working fluid for a given heat reservoir requires a multi-dimensional optimization method; some of the optimization parameters are not even physical or technical ones (Chen *et al.*, 2010, Bao and Zhao, 2013, Macchi and Astolfi, 2016).

Proper multi-dimensional optimization can only be performed when all of the sub-processes (dealing with one criterion) are adequately executed. Therefore, it is necessary to improve the various steps of the complex process of working fluid selection. We are focusing on one segment of this optimization method, related to the selection of the proper working fluid to avoid wet or superheated vapour states at the end of the expansion process. Starting the expansion from a saturated vapour state and using wet working fluid, the expansion is terminated in a mixed-phase state, in the so-called wet vapour region. Here, the vapour contains dispersed liquid (droplets), which can cause loss of efficiency as well as damage of expander due to droplet erosion. To avoid erosion problems, one can use a droplet separator device to remove the liquid part. Also, it is possible to apply superheating (i.e. increase of the fluid temperature from the saturated vapour state to a superheated dry vapour state); in this case, an additional heat exchanger section (superheater) is needed. Using dry fluid and starting the expansion from a saturated vapour state, the expansion has to be terminated in a low-temperature superheated dry vapour

state. Here, some residual heat has to be removed from the working fluid before condensation. This can cause some problems, including loss of efficiency or high cooling load of the condenser. To avoid these problems, one might choose the inclusion of an extra heat exchanger, called recuperator, which cools the superheated vapour before reaching the condenser and preheats the liquid (i.e. recovers some of the lost heat) before reaching the evaporator. The best solution would be the application of an isentropic working fluid, where ideal adiabatic expansions could run along (or nearby) the saturated vapour states during the whole expansion process. In this case a simple set-up of two heat exchangers, a pump and an expander could be sufficient to convert the heat to work by ORC. Unfortunately, such an ideal isentropic material does not exist; all real fluids classified as isentropic one have a reverse S-shaped saturated vapour branch on *T-s* diagram, not a the straight line with infinite slope, assumed by isentropicity. This is also true for fluids described by various molecular or equation of state based models (Garrido *et al*., 2012, Groniewsky *et. al.* 2017, Albornoz *et al*., 2018, Groniewsky and Imre, 2018, Györke *et al*., 2018, White and Velasco, 2018, White and Velasco, 2019).

Using our method, one can select a real, one-component working fluid from a database (Györke *et al*. 2019), with an ideal adiabatic (isentropic) expansion process starting from a saturated vapour state and terminating also in a saturated vapour state (or at least in the vicinity of this state), utilizing the "belly" of the reverse S-shaped saturated vapour branches of various materials. In this way, one can use the simplest ORC layout, consisting of only a pump, two heat exchangers (evaporator, condenser) and an expander, avoiding the use of superheater or droplet separator and a recuperative heat exchanger (recuperator). Since the fluid is always in dry condition during expansion, droplet erosion of the expander can also be avoided. Concerning the description of different set-ups used with various working fluids, more details can be seen for example in Macchi and Astolfi (2016) or in Groniewsky *et al*. (2017).

Presently, we have a database of around 30 pure fluids with *T-s* data taken from the NIST Chemistry Webbook (2018) and from RefProp 9.1 (2013). Most of these fluids were termed formerly as dry and a very few of them as isentropic, while in the novel classification they are in various isentropic sub-classes, namely in ANCMZ, ACNMZ, ANZCM and ANCZM.

From the present working fluid set, one can choose the thermodynamically most suitable material for a given ORC-cycle. Due to the temperature range covered by the *T-s* data, these fluids should be proper candidates mostly for cryogenic cycles, but after proper expansion, the database will be available for other temperature ranges (like geothermal or waste heat applications) as well.

## 2. MAPPING OF POTENTIAL EXPANSION ROUTES

According to the novel classification scheme, working fluids are classified by the entropy-sequences of their so-called primary and secondary characteristic points on the *T-s* diagram:

- Points A and Z are the initial and final points of the *T-s* saturation curve. Physically it is related to the triple point (or freezing point)
- Point C is the critical point, located on the top of the curve, separating the liquid branch (A-C) and the vapour branch (C-Z)
- Points M and N are local or global entropy extrema, located on the vapour branch.

Points A, Z and C exist for all working fluids (these are the primary points), while M exists only for dry and isentropic ones and N exists only for isentropic ones (therefore these are the secondary points). Theoretically, eight different classes can exist, one of them is wet (ACZ), two of them are dry (ACZM and AZCM) and five of them are "real" isentropics, with reverse S-shaped vapour branch (ANZCM, ANCZM, ANCMZ, ACNMZ and ACNZM). Concerning real materials, examples can be found only for six of these classes, neither ACZM, nor ACNZM have been found up to now. Some of these real isentropic materials (characterized by five-letter sequences) were considered formerly as dry ones, being the point N well below ambient temperatures. Using this classification, one can easily correlate material properties with the classification, i.e. separate wet and dry working fluids (Györke *el al*. 2019). Also, it can be used easily to study the behaviour of working fluids during the expansion process of ORC and other similar cycles (Imre and Groniewsky, 2019).

The above mentioned reverse S-shape allows us to define isentropic expansion routes. Two different *T-s* diagrams are shown in Figure 1: 2-methylbutane (a), heptane (b). It can be seen, that although none of them is real isentropic working fluid, one can still define isentropic expansion routes starting and

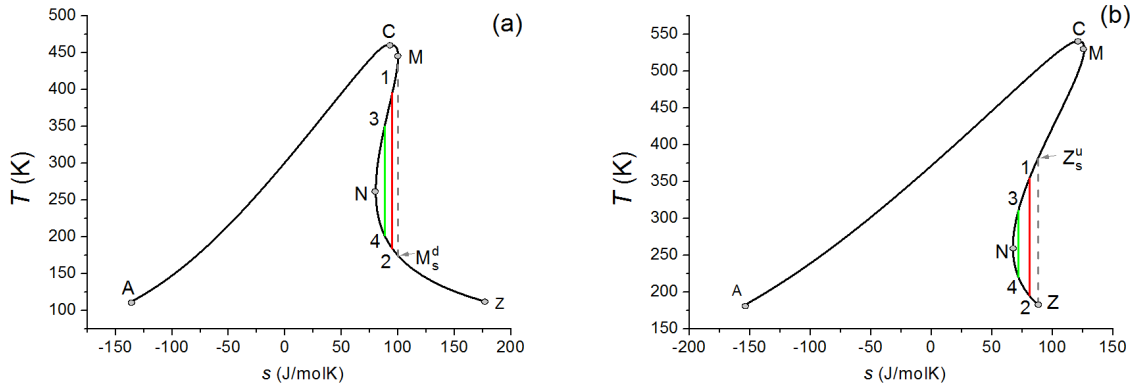


**Figure 1:** Potential isentropic expansion routes (1→2 and 3→4) for working fluids classified as ANCMZ (a; 2-methylbutane) and as ANZCM (b; heptane). Limiting expansion curves marked by dashed grey lines from $M \rightarrow M_s^d$ (a) and $Z_s^u \rightarrow Z$ (b).

terminating on the saturated vapour branch; these routes are marked as 1⟶2 and 3⟶4. For both materials, all potential isentropic expansion routes located in a "bay", separated by a limiting expansion line (grey dotted one) from the rest of the diagram. For ANCMZ-type working fluids, the limiting line is defined by the $M \rightarrow M_s^d$ expansion route; this is also true for ACNMZ-types. For ANZCM types, the limiting line is defined by the $Z_s^u \rightarrow Z$ expansion route; the same is true for ANCZM types.

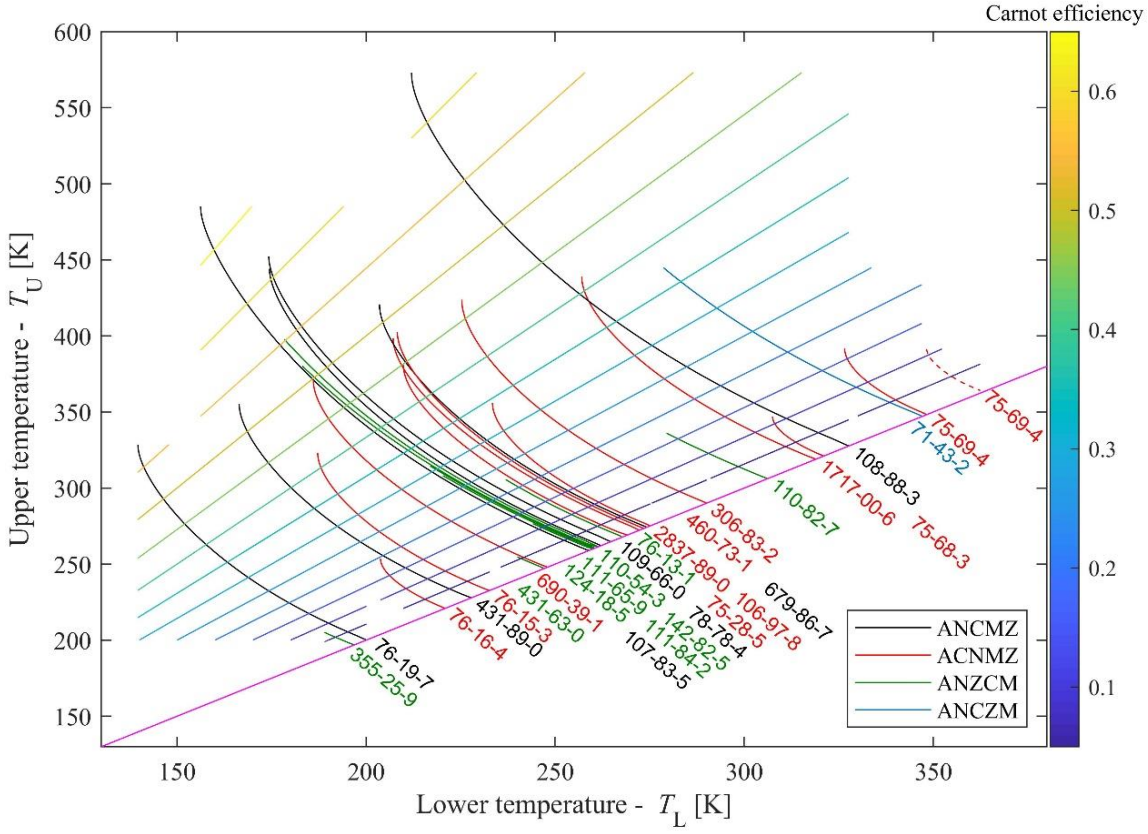


**Figure 2:** Potential isentropic expansion routes on $T_L$-$T_U$ diagram for 28 working fluids, identified by their CAS-number. Carnot-efficiencies for a given upper and lower temperature pair are given by color-coded lines.

**Table 1:** List of materials used in the study. The list is following the order of Figure 2 starting at 355-25-9 to 75-69-4.

| CAS-number | Name | R-number | Class |
|---|---|---|---|
| 355-25-9 | decafluorobutane | - | ANZCM |
| 76-19-7 | perfluoropropane | R218 | ANCMZ |
| 76-16-4 | freon 116 | R116 | ACNMZ |
| 431-89-0 | propane, 1,1,1,2,3,3,3-heptafluoro- | R227ea | ANCMZ |
| 76-15-3 | freon 115 | R115 | ACNMZ |
| 431-63-0 | 1,1,1,2,3,3-hexafluoropropane | R236ea | ANZCM |
| 690-39-1 | 1,1,1,3,3,3-hexafluoropropane | R236fa | ACNMZ |
| 107-83-5 | 2-methylpentane (isohexane) | - | ANCMZ |
| 124-18-5 | decane | - | ANZCM |
| 111-84-2 | nonane | - | ANZCM |
| 111-65-9 | octane | - | ANZCM |
| 142-82-5 | heptane | - | ANZCM |
| 110-54-3 | hexane | - | ANZCM |
| 78-78-4 | 2-methylbutane (isopentane) | R601a | ANCMZ |
| 109-66-0 | pentane | R601 | ANCMZ |
| 76-13-1 | freon 113 | R113 | ANZCM |
| 75-28-5 | 2-methylpropane (isobutane) | R600a | ACNMZ |
| 106-97-8 | butane | R600 | ACNMZ |
| 2837-89-0 | freon 124 | R124 | ACNMZ |
| 679-86-7 | 1,1,2,2,3-pentafluoropropane | R245ca | ANCMZ |
| 460-73-1 | 1,1,1,3,3-pentafluoropropane | R245fa | ACNMZ |
| 306-83-2 | freon 123 | R123 | ACNMZ |
| 110-82-7 | cyclohexane | - | ANZCM |
| 1717-00-6 | 1,1-dichloro-1-fluoroethane | R141b | ACNMZ |
| 75-68-3 | ethane, 1-chloro-1,1-difluoro- | R142b | ACNMZ |
| 108-88-3 | toluene | - | ANCMZ |
| 71-43-2 | benzene | - | ANCZM |
| 75-69-4 | trichlorofluoro-methane | R11 | ACNMZ |

Here, $Z_s^u$ and $M_s^d$ are the so-called tertiary characteristic points, marking the intersection on the saturation curve projecting the primary and secondary ones. Subscript s refers to the route of the projection (to the s-axis), while superscript u and d refers to the relative location compared to the original point (u: up; d: down).

Concerning the *T-s* diagrams used here, the specific entropy values are given for moles, instead of mass (i.e. in J/molK, instead of J/kgK). Although it is not usual in engineering applications, it has been shown recently, that for the comparison of various working fluids, the mole-based quantities are more suitable than the mass-based ones (Györke *et al*., 2019).

Within this bay, it is possible to define a $T_U$-$T_L$ curve for each material, where each point of this curve marks one potential isentropic expansion route between an upper (U) and lower (L) temperature. Using 28 materials with reverse S-shaped vapour branch and with *T-s* diagrams available in the NIST

databases (NIST Chemistry Webbook (2018) and from RefProp 9.1 (2013)), one can construct a map for all potential routes; this map is shown in Figure 2.

The lower end for all lines are on one curve, defined by the N-points; for the shortest possible expansion route $T_U=T_N+\delta$ and $T_L=T_N+\delta$, where $T_N$ refers to the temperature corresponding to point N and $\delta$ is an infinitesimally small temperature difference with $\delta \rightarrow 0$. For this reason, the lower limit should be located on a straight line with slope=1, where $T_U=T_N=T_L$. Marking this lower limit, one can avoid unrealistic $T_L>T_U$ cases.

Materials are identified by their chemical identifier (CAS number). When lines are congested, labels are following the order of lines in zig-zag. Materials corresponding to various classes are plotted in various colors; black for ANCMZ, red for ACNMZ, green for ANZCM and blue for ANCZM; as it was already mentioned, materials with ACNZM sequences have not been found up to now. For additional information, Carnot-efficiencies for a given upper and lower temperature pair are given by color-coded lines. The list of materials with their CAS-number, name, refrigerant code (if any) and classification can be found in Table 1.

Since *T-s* data are available in various sources, NIST-based data (NIST Chemistry Webbook (2018) and RefProp 9.1 (2013)) has been cross-checked. Visible difference was found only in one occasion (CAS 75-69-4, trichloromonofluoromethane, also called R11 or Freon 11); the alternative curve (data are taken from FluidProp (2016), using TPSI model, based on the work of Reynolds (1979)) is also plotted by the dashed red line.

## 3. HOW TO CHOOSE THE PROPER WORKING FLUID

Concerning an existing heat reservoir, one has to use a fixed maximal or upper temperature ($T_U$) for the cycle, given by the heat source temperature ($T_{source}$) and the pinch temperature ($\Delta T$, a characteristic value for the heat exchanger) as:

$$T_U = T_{source} - \Delta T \quad (1).$$

In a similar manner, the lowest temperature of the cycle ($T_L$) can be defined by the temperature of the environment used for cooling ($T_{environment}$) and a lower pinch temperature (not necessarily equal with the other one) as:

$$T_L = T_{environment} + \Delta T \quad (2).$$

This ($T_U$; $T_L$) pair can be used as a characteristic point in Figure 2 to represent a given heat source and sink with other technical details such as quality of heat exchangers.

In Figure 3/c, the grey cross represents the heat source and sink characterized by $T_U$=293 K= 20 ˚C and $T_L$=393 K= 120 ˚C. This can be for example a geothermal heat reservoir with a natural cold water source (a small river) or cold internal air (Winter) used for cooling. This situation is very similar to the first (and presently only) ORC-based Hungarian geothermal power plant (see the ORC Word Map, 2019).

In Figure 3/c, only part of the data presented in Figure 2 can be seen, centered on the (293K, 393 K) point. This point is located between two lines representing two working fluids, namely benzene (CAS 71−43−2) and toluene (CAS 108−88−3); one more material can be seen here, namely the 1,1−dichloro−1−fluoroethane (CAS 1717-00-6, also referred as R 141b). Since none of these lines run through the 293−392 K point, the closest ones (benzene and toluene) should be considered as nearest to ideal. The upper and lower temperature determines the extent of expansion, as it can be seen in Figure 3/a,d (benzene) and Figure 3/b,e (toluene).

For further discussion, we define the so-called quantity ($q$), also referred as dryness or dryness fraction of pure fluids, representing the ratio of vapour within the two-phase region and defined as:

$$q = \frac{n^v}{n^l+n^v} \quad (3)$$

where $n^v$ and $n^l$ are the mole- (or alternatively, the mass-) fraction of the fluid in the vapour or liquid phase, respectively. This quantity can change between 1 (saturated vapour) and 0 (saturated liquid); outside of the two-phase region, it is usually not defined or defined as 1 (vapour states) or 0 (liquid states). This ratio can be also calculated by using the specific entropy values for the given mixed state and comparing it with the entropy values of the saturated liquid and vapour states at the same temperature (Imre *et al.* 2014).

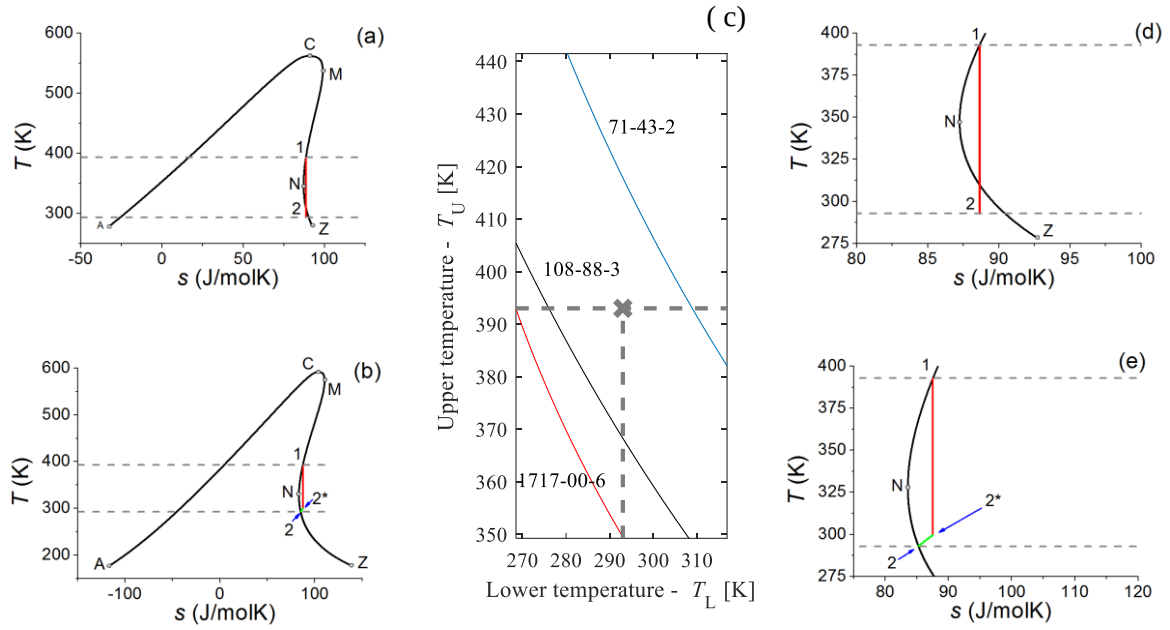


**Figure 3:** Expansion process for benzene, CAS 71-43-2 (a,d) and toluene, CAS 108-88-3 (b,e) for a given $T_L$-$T_U$ pair (293-393 K). Magnified part of Figure 2 centered on the 293-393 K point can be seen in the middle (c), representing benzene (blue) and toluene (black). Right-side figures (d and e) show the magnified parts for (a) and (b) around point N, for the better visibility of the expansion lines.

In the case of benzene (Figure 3/a and d), one can see that the expansion route started at saturated vapour state at 393 K and terminated at 293 K, runs in superheated dry vapour region for a while, but the final part of the expansion (starting from 309.96 K down to 292 K, i.e. in an almost 18 K temperature range) runs into the two-phase, wet region. The maximal $q$ value (corresponding to the final state of the expansion) is 0.9846, equal to 1.54 % (in mass) of droplet. Droplets may cause erosion problems, moreover they might decrease the net efficiency due to moisture loss, although this 1.54% is not very high compared to the 8-12 % which is usually considered tolerable (Bassily, 2005). For benzene, the ideal case – i.e. expansion from one saturated vapour state to an other saturated vapour state – would be the termination of expansion at $T_L$= 309.96 K, given by the cross section of the blue line (representing benzene) and grey dashed line (representing $T_U$=393 K). Stopping at this higher temperature would cause smaller efficiency, therefore the problem of droplet erosion should be weighted against the problem of potential efficiency loss, before deciding the use or omission of benzene. It also means that benzene would be the ideal working fluid (concerning expansion route) for a heat source and sink characterized by ($T_U$, $T_L$)=(393 K, 309.96 K) temperatures.

In case of toluene (Figure 3/b and e) if the expansion route starts at saturated vapour state at 393 K and terminates at 293 K, than even the final part of the expansion runs in superheated dry vapour states. Therefore one would not face challenges regarding droplet formation. Unfortunately, an other problem emerges, namely the problem of cooling down the expanded dry vapour in an isobaric way before reaching saturated vapour state at $T_L$=293 K. Therefore, isentropic expansion (solid red line) has to be stopped at a higher temperature (point 2*) and the rest of the process (2*→2) has to proceed on an isobaric cooling route (green line). In this way, a small, almost triangle shaped part in the $T$-$s$ diagram (formed by the grey line, the green line and by the extension of the red one) will be excluded from the cycle, decreasing the thermal efficiency. As an additional problem, this unused (lost) heat can increase the heat-load of the environment. Addition of a recuperative heat exchanger to the system can solve – or at least minimize – these problems, since part of this heat can be used to pre-heat the compressed liquid. This solution is appropriate only if the temperature difference between point 2* and 2 is large enough. In case of toluene with 393-293 K expansion, this gap is around $\Delta T$=9 K, which can be used only in a very limited manner for this purpose. With a larger gap, this heat can be utilized better,

however the thermal efficiency is still smaller, therefore the goal remains to reach a perfect "saturated steam to saturated steam" expansion route, with zero gap. Similarly to the case of benzene, one can define an ideal $T_L$, where expansion from $T_U$ would be terminated at the saturated vapour state; for toluene it would be 276.06 K. It means, that toluene would be the ideal working fluid (concerning expansion route) for a heat source and sink characterized by ($T_U$, $T_L$)=(393 K, 276.06 K) temperatures. Unfortunately, none of the expansion routes of known working fluids run through the (393 K, 293 K) point, therefore one can choose only something "close enough". An other alternative would be – especially when there are two "close enough" working fluids with chemically similar structure –the application of a mixture. Due to the chemical similarity, the mixture would be probably an almost ideal, zeotropic mixture, which can be used more easily as working fluid in ORC applications than azeotropic ones (Albornoz et al., 2018, Su *et al.*, 2018, Varga and Csaba, 2018).

Concerning lower temperatures, one can see regions on the $T_U$-$T_L$ diagram densely packed with expansion routes. Recently, there are more and more applications for liquid methane (LNG). LNG can be transported to LNG-terminals by ships, and there they must be re-gasified before injected into the regular gas network. Concerning the fact, that the temperature of liquid methane can be as low as 111 K (-162 ˚C), the external heat used for re-gasification can be even the environmental heat (air, water), around or below 300 K. Obviously, going down to 111 K in an ORC would cause some serious problems concerning materials used for the construction, but using the methane as heat sink and cooling the chosen working fluid down only to a moderate level, one can define an acceptable expansion range for example between $T_U$=303 K and $T_L$=228.5 K. In Figure 4/a, one can see part of Figure 2 centered around this point. It is clearly visible, that one line runs almost exactly through this point, namely the line representing 2-methylbutane (isopentane, CAS 78-78-4) and it is slightly off from the lines representing

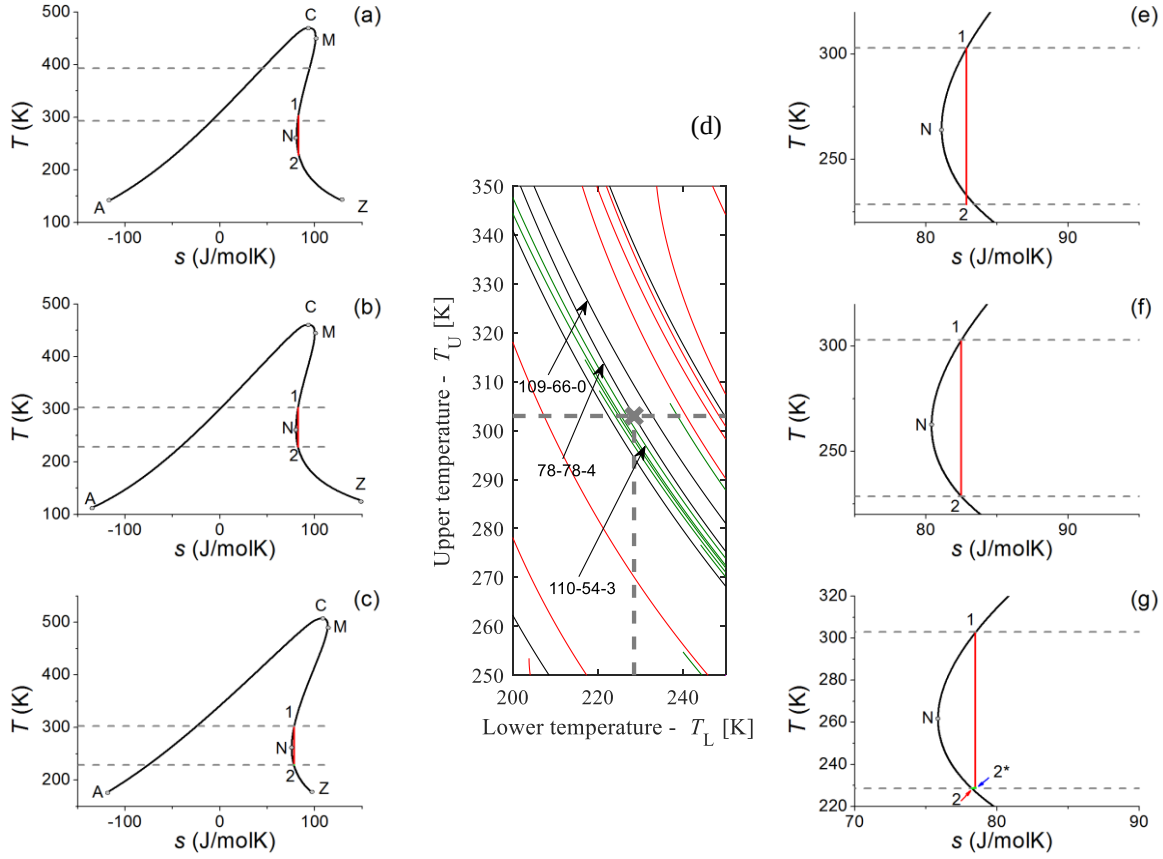


**Figure 4:** Expansion process for pentane (CAS 109-66-0) (a,e), 2-methylbutane (CAS 78-78-4) (b,f) and hexane (CAS 110-54-3) (c,g) for a given $T_L$-$T_U$ pair (228.5 K, 303 K)). Magnified part of Figure 2 centered on the 228.5-303 K point can be seen in the middle (d), representing the expansion routes for pentane black), 2-methylbutane (black) and hexane (green). Right-side figures (e,f and g) show the magnified parts for (a), (b) and (c) diagrams, for the better visibility of the expansion lines.

two linear alkanes, hexane (CAS 110-54-3) and pentane (CAS 109-66-0). Expansion lines for these three working fluids are shown in Figure 4/a and e (pentane), Figure 4/b and f (2-methylbutane) and Figure 4/c and g (hexane).

First, the potential use of pentane is discussed. In this case, the end of the expansion runs into the two-phase (wet) region (see Figure 4/a and e), but in a much smaller extent, than it was shown for benzene. Here, the expansion line enters the two-phase region around 232.8 K, only 4.3 K above the end of the expansion process. The quality of wet steam will be 0.9924, corresponding to 0.76 % wetness, half of the value reported in the previous case. In the case of benzene, the wetness was already in the tolerable level; it is even more valid for this case.

By using 2-methylbutane, the expansion between $T_U$=303 K and $T_L$=228.5 K starts and terminates in saturated vapour states, avoiding all problem related to wet or superheated dry vapour. This is shown in Figure 4/b and f. Concerning the expansion route, this is the perfect working fluid for a heat source and heat sink pair, represented by $T_U$=303 K and $T_L$=228.5 K.

Finally, the use of hexane is discussed. In this case, the expansion should be terminated within the dry vapour region and the working fluid has to be cooled down to $T_L$ by isobaric cooling. Here, the isobaric part is so small, that it can be hardly seen even on the magnified figure (Figure 4/g); the expansion has to stop at 228.97 K, instead of 228.5 K, only 0.47 K above the $T_L$. This small gap cannot be utilized for pre-heating the pressurized liquid, but the heat loss caused by this part is negligible.

In the case of $T_U$=303 K and $T_L$=228.5 K, one can pinpoint the ideal working fluid, where expansion would run from one saturated vapour state to an other saturated vapour state, all along a dry vapour route. At the end of the expansion, the final state would be a saturated vapour state, therefore the problems caused by wet or superheated dry vapour (discussed above) do not exist! This ideal working fluid would be the 2-methylpentane. Due to the fact that expansion routes for several materials run in the immediate vicinity of this ($T_U$, $T_L$)=(228.5 K, 303 K) point, one can even found a second-, third-, fourth-best. Because these routes are close to our working point, using one of them – instead of the ideal one – would cause only minor problems, acceptable for the given application. For this temperature range, the ones next to the best would be pentane and hexane; using them the problems caused by the presence of droplets or superheated dry vapour are almost negligible, therefore their application (and probably the application of several other working fluids with expansion range lines running close to the ($T_U$, $T_L$)=(228.5 K, 303 K)) would be acceptable. In this way, one could use other criteria (environmental safety, chemical compatibility, price, availability, etc.) together with some optimization method (see for example Quoilin *et al*., 2013 and Zhang *et al*., 2014, Shi and Pan, 2019) to choose the proper working fluid, still acceptable thermodynamically, but not necessarily the best one according to this criterion.

## 6. CONCLUSIONS

A novel method has been proposed to choose the best working fluid – from the point of view of expansion route – for a given heat source and heat sink (characterized by a maximum and minimum temperature). The proposed method can be used as part of the multi-dimensional working fluid selection process, focusing on one of the important criteria. The method is based on the novel classification of working fluids using the sequences of their characteristic points on temperature-entropy space (Györke *et al.*, 2018). Using this method, we are able to select a working fluid (from a database, see Györke *et al*. 2019), where an ideal adiabatic (isentropic) expansion process between a given upper and lower temperature is possible in a way, that the initial and final states are both saturated vapour states and the ideal (isentropic) expansion line runs in the superheated dry vapour region all along the expansion. In this way, it is possible to avoid problems related to the presence of droplets or superheated dry steam in the final expansion state, just before the condensation. Therefore, one can use the most simple ORC layout, using only a pump, two heat exchangers (evaporator, condenser) and an expander, avoiding the use of superheater (or droplet separator) and recuperator; since the fluid is always in dry condition during expansion, droplet erosion can also be avoided.

Presently we have a database of nearly 30 pure fluids with *T-s* data taken from the NIST Chemistry Webbook (2018) and from RefProp 9.1 (2013). Most of these fluids were termed formerly as “dry”, while in the novel classification they are in various isentropic sub-classes, namely in ANCMZ,

ACNMZ, ANZCM and ANCZM. Due to the fact, that the characteristic point responsible for the existence of these expansion routes (point N) is usually located at low temperature for most of the materials of our database, presently this method can mostly be used to choose the working fluids thermodynamically most suitable for cryogenic cycles (applied for example for heat recovery during LNG-regasification, see for example Sadaghiani *et al.*, 2018 and Atienza-Márquez *et al.*, 2019 ), although some of the materials can be used in higher temperatures (covering part of the temperature range for geothermal and waste heat utilization).
Extension of the method (including internal efficiencies below 1 for the expander as well as acceptable wetness for the final vapour state) and expansion of the database with more material are in progress. After a proper extension of the database, this method will be available to choose ideal working fluids for other temperatures (like the ones characteristic for various geothermal or waste heat applications).

## NOMENCLATURE

| | | |
|---|---|---|
| A, N, C, Z, M | various characteristic point of saturation curves in temperature-entropy space | |
| CAS | Chemical Abstracts Service registry number | |
| $\delta$ | infinitesimal temperature difference | (K) |
| $n$ | mole ratio | (–) |
| NIST | National Institute of Standard and Technology, USA | |
| ORC | Organic Rankine Cycle | |
| $q$ | quantity or dryness ratio | (–) |
| R | refrigerant number | |
| $s$ | specific entropy | (J/molK or J/kgK) |
| $T$ | temperature | (K or ˚C) |
| $T$-$s$ | temperature-specific entropy diagram | |

**Subscript**

| | |
|---|---|
| d, u | down, up |
| l, v | liquid, vapour |
| L, U | lowest, uppermost (in temperature) |
| N | related to point N |
| s | projection to the specific entropy axis |

## REFERENCES

Albornoz, J., Mejía, A., Quinteros-Lama, H., Garrido, J.M., 2018, A rigorous and accurate approach for predicting the wet–to–dry transition for working mixtures in organic Rankine cycles, *Energy*, vol. 156, pp. 509–519.

Atienza-Márquez, A., Bruno, J.C., Akisawa, A., Nakayama, M., Coronas, A., 2019, Fluids selection and performance analysis of a polygeneration plant with exergy recovery from LNG regasification, *Energy*, accepted manuscript, doi: https://doi.org/10.1016/j.energy.2019.04.060.

Bao, J., Zhao, L., 2013, A review of working fluid and expander selections for Organic Rankine Cycle, Renew. Sustain. Energy Rev. vol. 24, pp325–342.

Bassily, A.M., 2005, Modeling, numerical optimization, and irreversibility reduction of a dual-pressurere heat combined-cycle, *Applied Energy*, vol. 81, pp. 127–151.

Blaise, M.; Feidt, M., 2019, Waste Heat Recovery and Conversion into Electricity: Current Solutions and Assessment, International Journal of Thermodynamics, vol. 22, pp. 1–7.

Chen, H., Goswami, D.Y., Stefanakos, E.K., A review of thermodynamic cycles and working fluids for the conversion of low–grade heat, *Renew. Sustain. Energy Rev*. vol. 14, pp.3059–3067.

FluidProp version 3.0.4., 2016, http://www.asimptote.nl/software/fluidprop/

Garrido, J.M., Quinteros-Lama, H., Mejía, A., Wisniak, J., Segura, S., 2012, A rigorous approach for predicting the slope and curvature of the temperature–entropy saturation boundary of pure fluids, *Energy*, vol. 45, pp. 888–899.

Groniewsky, A., Györke, G., Imre, A.R., 2017, Description of wet-to-dry transition in model ORC working fluids, *Applied Thermal Engineering*, vol. 125, pp. 963–971.

Groniewsky, A., Imre, A.R., 2018, Prediction of the ORC working fluid's temperature-entropy saturation boundary using Redlich-Kwong equation of state, *Entropy*, vol. 20, #93.

Györke, G., Deiters, U.K., Groniewsky, A., Lassu, I., Imre, A.R., 2018, Novel Classification of Pure Working Fluids for Organic Rankine Cycle, *Energy*, vol. 145, pp. 288–300.

Györke, G., Groniewsky, A., Imre, A.R., 2019, A simple method to find new dry and isentropic working fluids for Organic Rankine Cycle, *Energies*, vol. 12, #480.

Imre, A.R., Quinones-Cisneros, S.E., Deiters, U.K., 2014, Adiabatic processes in the liquid–vapor two–phase region – 1. Pure fluids, *Industrial&Engineering Chemistry Research*, vol. 53, pp. 13529–13542.

Imre, A.R., Groniewsky, A., 2019, Various ways of adiabatic expansion in Organic Rankine Cycle (ORC) and in Trilateral Flash Cycle (TFC), *Zeitschrift für Physikalische Chemie*, vol. 233, pp. 577–594.

Macchi, E., Astolfi, M. (editors), 2016, Organic Rankine Cycle (ORC) power systems: technologies and applications. Elsevier.

NIST Chemistry WebBook, 2018, NIST Standard Reference Database Number 69, http://webbook.nist.gov/chemistry/.

ORC World Map, 2019, https://orc-world-map.org/

Quoilin, S., Van Den Broek, M., Declaye, S., Dewallef, P., Lemort, V., 2012, Technoeconomic survey of Organic Rankine Cycle (ORC) systems, Renew. Sustain. Energy Rev. vol. 22, pp. 168–186.

RefProp 9.1, 20013, https://www.nist.gov/srd/refprop

Reynolds, W.C., Thermodynamic properties in S.I., 1979, Department of Mechanical Engineering - Stanford University, Stanford, CA.

Sadaghiani, M.S., Ahmadi, M.H., Mehrpooya, M., Pourfayaz, P., Feidt, M., 2018, Process development and thermodynamic analysis of a novel power generation plant driven by geothermal energy with liquefied natural gas as its heat sink, *Applied Thermal Engineering*, vol. 133, pp. 645–658.

Shi, W., Pan, L., 2019, Optimization Study on Fluids for the Gravity-Driven Organic Power Cycle, *Energies*, vol. 12, #732

Su, W., Hwang, Y., Deng, S., Zhao, L., Zhao, D., 2018, Thermodynamic performance comparison of Organic Rankine Cycle between zeotropic mixtures and pure fluids under open heat source, *Energy Conversion and Management*, vol. 165, pp. 720-737.

Varga, Z.; Csaba, T., 2018, Techno-economic evaluation of waste heat recovery by organic Rankine cycle using pure light hydrocarbons and their mixtures as working fluid in a crude oil refinery, *Energy Conversion and Management*, vol. 174, pp. 793-801.

White, J.A., Velasco, S., 2018, Characterizing wet and dry fluids in temperature-entropy diagrams, *Energy*, vol. 154, pp. 269-276.

White, J.A., Velasco, S., 2019, A Simple Semiempirical Method for Predicting the Temperature−Entropy Saturation Curve of Pure Fluids, *Industrial&Engineering Chemistry Research*, vol. 58, pp. 1038-1043.

Zhang, X., He, M., Wang, J., 2014, A new method used to evaluate organic working fluids, *Energy*, vol. 67, pp. 363-369.

## ACKNOWLEDGEMENT

This work was performed in the frame of FIEK_16-1-2016-0007 project, implemented with the support provided from the National Research, Development and Innovation Fund of Hungary, financed under the FIEK_16 funding scheme. Some part of the research reported in this paper was supported by the Higher Education Excellence Program of the Ministry of Human Capacities in the frame of Nanotechnology research area of Budapest University of Technology and Economics (BME FIKP-NANO) Partial financial supports of the Hungarian National Innovation Office grant (NKFIH, grant No. K116375) is also acknowledged.